A structure-based model with stropholysis effects

By S. C. Kassinos AND W. C. Reynolds

1. Motivation and objectives

The performance of Reynolds Stress Transport (RST) models is limited by the lack of information about two dynamically important effects: the role of energy-containing turbulence structure (dimensionality) and the breaking of reflectional symmetry (stropholysis) due to strong mean or frame rotation. Both effects are fundamentally nonlocal in nature and this explains why it has been difficult to include them in *one-point* closures such as RST models. Information about the energy-containing structure is necessary if turbulence models are to reflect differences in dynamic behavior associated with structures of different dimensionality (nearly isotropic turbulence *vs.* turbulence with strongly organized two-dimensional structures). Information about the breaking of reflectional symmetry is important whenever mean rotation is dynamically important (flow through axisymmetric diffuser or nozzle with swirl, flow through turbomachinery, etc.).

Engineering flows that must now be computed to advance technology require that dimensionality and stropholysis effects be properly captured in one-point closures. The information needed in order to address these issues is carried by new one-point tensors whose definitions and transport equations were obtained in earlier work (Kassinos and Reynolds 1994). Two of these tensors, the dimensionality D_{ij} and circulicity F_{ij}, characterize the energy-containing structure. Another tensor, the third-rank fully symmetric stropholysis Q^*_{ijk}, parameterizes the breaking of reflectional symmetry in the spectrum of turbulence. Reflectional symmetry breaking is not properly captured in second-rank tensors such as the Reynolds stresses R_{ij} or even D_{ij} and F_{ij}.

In our ongoing effort to construct one-point structure-based models for engineering use, we have in the past formulated a simplified nonlocal theory for the deformation of homogeneous turbulence, the Interacting Particle Representation Model or IPRM (see Kassinos and Reynolds 1996). The IPRM gives excellent results for general deformations of homogeneous turbulence and has been helping us formulate one-point models. A one-point model (the *R-D* model described in Kassinos and Reynolds 1997) was formulated using the IPRM ideas and produces excellent results for both rapid and slow *irrotational* deformation of homogeneous turbulence. The *R-D* model cannot be applied to flows with strong mean or frame rotation because it lacks important physics related to stropholysis $\mathbf{Q}^*$.

In the past year, we have formulated a new one-point model, the Q-model, which is based on our understanding of the stropholysis effects and which uses the effective gradients model from the IPRM (see Kassinos & Reynolds 1996) for the modeling of nonlinear effects. For irrotational deformations the Q-model is equivalent to the previously formulated *R-D* model (see Kassinos & Reynolds 1997) and produces

good results for both rapid and slow mean deformations. The Q-model overcomes the restriction to irrotational deformation that applied to the previous model and produces good results even for flows with combinations of strong mean rotation and strain.

The development of the Q-model is an ongoing effort, and we expect that some aspects of the model will eventually be modified, but this preliminary note sketches the basic ideas.

2. Accomplishments

2.1 Why stropholysis-based models?

One-point models based directly on stropholysis transport have certain important advantages. The stropholysis tensor contains information stemming from the breaking of reflectional symmetry in the spectrum of turbulence that has undergone mean rotation. This information is not contained in second-rank tensors such as the Reynolds stress tensor or even the dimensionality D_{ij} and circulicity F_{ij}. This means that models based on these second-rank tensors, including standard Reynolds Stress Transport (RST) models, must be supplemented with ad-hoc phenomenological models in order to emulate even the leading order effects of stropholysis. The use of ad-hoc models for stropholysis in these lower-rank models eliminates any hope of achieving good realizability properties under non-equilibrium conditions. The added computational cost for carrying a third-rank equation might be a reasonable price to pay if stropholysis-based models can capture subtle rotational effects while maintaining good realizability properties. The model described here is a first attempt at exploring these ideas.

2.2 Definitions and constitutive equations

We introduce the turbulent stream function Ψ'_i, defined by

$$u'_i = \epsilon_{its}\Psi'_{s,t} \qquad \Psi'_{i,i} = 0 \qquad \Psi'_{i,nn} = -\omega'_i\,, \tag{1}$$

where u'_i and ω'_i are the fluctuating velocity and vorticity components. The Reynolds stress tensor and the associated nondimensional and anisotropy tensors are defined by

$$R_{ij} = \overline{u'_i u'_j} = \epsilon_{ipq}\epsilon_{jts}\overline{\Psi'_{q,p}\Psi'_{s,t}}\,, \qquad r_{ij} = R_{ij}/q^2, \qquad \tilde{r}_{ij} = r_{ij} - \tfrac{1}{3}\delta_{ij}\,. \tag{2}$$

Here $q^2 = 2k = R_{kk}$. Introducing the isotropic tensor identity (Mahoney 1985)

$$\epsilon_{ipq}\epsilon_{jts} = \delta_{ij}\delta_{pt}\delta_{qs} + \delta_{it}\delta_{ps}\delta_{qj} + \delta_{is}\delta_{pj}\delta_{qt} - \delta_{ij}\delta_{ps}\delta_{qt} - \delta_{it}\delta_{pj}\delta_{qs} - \delta_{is}\delta_{pt}\delta_{qj} \tag{3}$$

one finds

$$R_{ij} + \underbrace{\overline{\Psi'_{k,i}\Psi'_{k,j}}}_{D_{ij}} + \underbrace{\overline{\Psi'_{i,k}\Psi'_{j,k}}}_{F_{ij}} - \underbrace{\overline{\Psi'_{i,k}\Psi'_{k,j}} + \overline{\Psi'_{j,k}\Psi'_{k,i}}}_{C_{ij}+C_{ji}} = \delta_{ij}q^2\,. \tag{4}$$

The constitutive Eq. (4) shows that one-point correlations of stream function gradients, such as the Reynolds stresses, are dominated by the energy-containing scales. These correlations contain independent information that is important for the proper characterization of non-equilibrium turbulence.

For homogeneous turbulence $C_{ij} = C_{ji} = 0$, and the remaining tensors in (4) have equivalent representations in terms of the velocity spectrum tensor $E_{ij}(\mathbf{k})$ and vorticity spectrum tensor $W_{ij}(\mathbf{k})$. These are as follows:
• Structure *dimensionality* tensor

$$D_{ij} = \int \frac{k_i k_j}{k^2} E_{nn}(\mathbf{k})\ d^3\mathbf{k} \qquad d_{ij} = D_{ij}/q^2 \qquad \tilde{d}_{ij} = d_{ij} - \tfrac{1}{3}\delta_{ij} \tag{5}$$

• Structure *circulicity* tensor

$$F_{ij} = \int \mathcal{F}_{ij}(\mathbf{k})\ d^3\mathbf{k} \qquad f_{ij} = F_{ij}/q^2 \qquad \tilde{f}_{ij} = f_{ij} - \tfrac{1}{3}\delta_{ij}\,. \tag{6}$$

Here $\mathcal{F}_{ij}(\mathbf{k})$ is the circulicity spectrum tensor, which is related to the vorticity spectrum tensor $W_{ij}(\mathbf{k}) = \overline{\hat{\omega}_i \hat{\omega}_j^*}$ through the relation

$$\mathcal{F}_{ij}(\mathbf{k}) = \frac{W_{ij}(\mathbf{k})}{k^2}.$$

The familiar rapid pressure−strain-rate term is given by

$$T_{ij} = 2G_{ts}(M_{istj} + M_{jsti}) \tag{7}$$

where the fourth-rank tensor $\mathbf{M}$ is

$$M_{ijpq} = \int \frac{k_p k_q}{k^2} E_{ij}(\mathbf{k})\ d^3\mathbf{k}\,. \tag{8}$$

We define the third rank tensor

$$Q_{ijk} = -\overline{u'_j \Psi'_{i,k}}\,. \tag{9}$$

For homogeneous turbulence, Q_{ijk} has the equivalent definition

$$Q_{ijk} = \epsilon_{ipq} M_{jqpk} \tag{10}$$

where M_{ijpq} is as in (8). The general definition of the third-rank fully symmetric *stropholysis* tensor is given by

$$Q^*_{ijk} = \frac{1}{6}(Q_{ijk} + Q_{jki} + Q_{kij} + Q_{ikj} + Q_{jik} + Q_{kji})\,. \tag{11}$$

In the case of homogeneous turbulence both Q_{ijk} and Q^*_{ijk} are bi-trace free

$$Q_{iik} = Q_{iki} = Q_{kii} = 0 \qquad Q^*_{iik} = 0\,. \tag{12}$$

A decomposition based on group theory shows that Q_{ijk} and Q^*_{ijk} are related to each other and lower-rank tensors,

$$Q_{ijk} = \tfrac{1}{6}q^2\epsilon_{ijk} + \tfrac{1}{3}\epsilon_{ikm}R_{mj} + \tfrac{1}{3}\epsilon_{jim}D_{mk} + \tfrac{1}{3}\epsilon_{kjm}F_{mi} + Q^*_{ijk}\,, \tag{13}$$

and

$$R_{ij} = \epsilon_{imp}Q_{mjp} \quad D_{ij} = \epsilon_{imp}Q_{pmj} \quad F_{ij} = \epsilon_{imp}Q_{jpm}\,. \tag{14}$$

2.1 IPRM formulation

Kassinos & Reynolds (1994, 1996) formulated a simplified nonlocal theory (Particle Representation Model or PRM) for the RDT of homogeneous turbulence. The original idea was to represent the turbulence by an ensemble of fictitious particles. A number of key properties and their evolution equations are assigned to each particle. Ensemble averaging produces a representation of the one-point statistics of the turbulent field, which is exactly correct for the case of RDT of homogeneous turbulence. In essence, this approach represents the simplest theory beyond one-point methods that provides closure for the RDT equations without modeling.

The Interacting Particle Representation Model (IPRM) is the more recent extension of the PRM formulation that includes the effects of the nonlinear eddy-eddy interactions, important when the mean deformations are slow. Unlike standard models, which use return-to-isotropy terms, the IPRM incorporates nonlinear effects through the use of effective gradients. The effective gradients idea postulates that the background nonlinear particle-particle interactions provide a gradient acting on each particle in addition to the actual mean velocity gradient. An advantage of this formulation is the preservation of the RDT structure of the governing equations even for slow deformations of homogeneous turbulence. A detailed account of these ideas is given in Kassinos & Reynolds (1996, 1997) and will not be repeated here. To a large extent, the one-point Q-model is based on the IPRM formulation.

The governing equations for the conditional (cluster averaged) IPRM formulation are (see Kassinos & Reynolds 1996)

$$\dot{n}_i = -G^n_{ki}n_k + G^n_{kr}n_k n_r n_i \tag{15}$$

$$\begin{aligned}\dot{R}^{|\mathbf{n}}_{ij} = &-G^v_{ik}R^{|\mathbf{n}}_{kj} - G^v_{jk}R^{|\mathbf{n}}_{ki} + [G^n_{km} + G^v_{km}](R^{|\mathbf{n}}_{im}n_k n_j + R^{|\mathbf{n}}_{jm}n_k n_i)\\ &- [2C_1R^{|\mathbf{n}}_{ij} - C_2^2R^{|\mathbf{n}}_{kk}(\delta_{ij} - n_i n_j)]\,.\end{aligned} \tag{16}$$

Here $n_i(t)$ is the unit gradient vector and $R^{|\mathbf{n}}_{ij}$ is the conditional Reynolds stress tensor corresponding to a cluster of particles with a common $n_i(t)$. The effective gradients are

$$G^n_{ij} = G_{ij} + \frac{C^n}{\tau}r_{ik}d_{kj} \qquad G^v_{ij} = G_{ij} + \frac{C^v}{\tau}r_{ik}d_{kj}\,. \tag{17}$$

where G_{ij} is the mean velocity gradient. The constants C^v and C^n are taken to be $C^n = 2.2C^v = 2.2$. The different values for these two constants account for the different rates of return to isotropy of D_{ij} and R_{ij}.

The turbulent time scale τ is chosen so as to produce the proper dissipation rate. The rate of dissipation of the turbulent kinetic energy $k = \frac{1}{2}q^2$ that is produced by the IPRM Eq. (16) is given by

$$\epsilon^{\rm PRM} = q^2 \frac{C^v}{\tau} r_{ik} d_{km} r_{mi} \,. \tag{18}$$

To complete the IPRM we use the standard model equation for the dissipation rate (ϵ) with a rotational modification to account for the suppression of ϵ due to mean rotation,

$$\dot{\epsilon} = -C_0(\epsilon^2/q^2) - C_s S_{pq} r_{pq} \epsilon - C_\Omega \sqrt{\Omega_n \Omega_m d_{nm}}\, \epsilon \,. \tag{19}$$

Here Ω_i is the mean vorticity vector, and the constants are taken to be

$$C_0 = 3.6 \qquad C_s = 3.0 \qquad \text{and} \qquad C_\Omega = 0.01 \,.$$

We choose the time scale τ so that $\epsilon^{\rm PRM} = \epsilon$. This requires that

$$\tau = (\frac{q^2}{\epsilon}) C^v r_{ik} d_{km} r_{mi} \,. \tag{20}$$

The last term in (16) accounts for rotational randomization due to eddy-eddy interactions. We require that the rotational randomization model leaves the conditional energy unmodified. This requires that $C_1 = C_2^2$, and hence using dimensional considerations we take

$$C_r = C_1 = C_2^2 = \frac{8.5}{\tau}\, \Omega^* \, f_{pq} n_p n_q \qquad \Omega^* = \sqrt{\Omega_k^* \Omega_k^*} \qquad \Omega_i^* = \epsilon_{ipq} r_{qk} d_{kp} \,. \tag{20}$$

2.3 The stropholysis equation

The most convenient method for deriving the slow $\mathbf{Q}$ equation is to use the conditional (cluster averaged) IPRM formulation to obtain the evolution equation for $\mathbf{M}$ and then contract the $\mathbf{M}$ equation with the alternating tensor ϵ_{ijk} to extract the $\mathbf{Q}$ equation†. The PRM representation for $\mathbf{Q}$ and $\mathbf{M}$ is

$$Q_{ijk} = -\langle V^2 v_j s_i n_k \rangle \qquad M_{ijpq} = \langle V^2 v_i v_j n_p n_q \rangle \tag{21}$$

where s_i is the unit stream function vector. Hence using (15) and (16) and the definitions (10) and (21) , one obtains

† To be precise, stropholysis is the fully symmetric subtensor $\mathbf{Q}^*$. Here we refer to the $\mathbf{Q}$ equation as the stropholysis information since $\mathbf{Q}$ contains the (stropholysis) information found in $\mathbf{Q}^*$.

$$\frac{dQ_{ijk}}{dt} = -G^v_{jm}Q_{imk} - G^n_{mk}Q_{ijm} - G^v_{sm}\epsilon_{its}M_{jmtk} - G^n_{mt}\epsilon_{its}M_{jsmk} + [G^n_{wq} + G^v_{wq}]Q_{iqwjk} + 2G^n_{qr}Q_{ijkqr} - \frac{8.5}{\tau}\,\Omega^*\, f_{rs}[Q_{ijkrs} + Q_{jikrs}]\,. \tag{22}$$

2.3 Closure of the stropholysis equation

Closure of (22) requires a model for the tensor Q_{ijkpq} in terms of Q_{ijk}. Once such a model has been specified, it effectively provides a model for M_{ijpq} in terms of Q_{ijk} since $\mathbf{M}$ can be obtained from Q_{ijkpq} by a contraction with ϵ_{ijk}. For small anisotropies, one can write an exact representation of Q_{ijkpq} in terms of Q_{ijk} that is linear in Q_{ijk}. Other tensors such as R_{ij}, D_{ij}, and F_{ij} can be expressed in terms of Q_{ijk} [see (14)] and need not be included explicitly in the model. Definitions (contractions and continuity) determine all the numerical coefficients in the linear model. Thus the linear model contains no adjustable parameters.

In the presence of mean rotation, *rotational randomization* is an important dynamical effect that must be accounted for in the model. Rotational randomization is a strictly nonlocal effect that is lost in the averaging procedure that generates one-point statistics. Rotational randomization is caused by the differential action of mean rotation on particle velocity vectors (Fourier modes) according to the alignment of the corresponding gradient (wavenumber) vectors with the axis of mean rotation. The main impact of Fourier randomization on one-point statistics is the damping of rotation-induced adjustments; here this effect is added explicitly through a simple model,

$$\frac{DQ_{ijk}}{Dt} = \ldots - \gamma_1(Q_{ijk} - Q^{rf}_{ijk}) - \gamma_2\,\epsilon_{ijm}(R_{mk} - D_{mk}) - \gamma_3\,\epsilon_{ikm}(F_{mj} - D_{mj})\,. \tag{23}$$

The first term accounts for the rotational randomization effects in rotation dominated flows while the remaining two terms account for the modification of these effects due to the combined action of mean strain and rotation. Here γ_1, γ_2 and γ_3 are scalar functions of the invariants of the mean strain and rotation and are determined from simple test cases. A detailed discussion of these models will appear separately.

2.4 Representative results for homogeneous turbulence

Examples of the performance of the new, one-point Q-model for irrotational mean deformation are shown in Figs. 1 and 2. A particularly interesting test case is that of homogeneous turbulence deformed by *slow* axisymmetric expansion (axisymmetric impingement). The mean velocity gradient tensor in this case is

$$S_{ij} = \frac{2}{\sqrt{3}}S\begin{pmatrix} -1 & 0 & 0 \\ 0 & \frac{1}{2} & 0 \\ 0 & 0 & \frac{1}{2} \end{pmatrix}, \qquad S = \sqrt{S_{ij}S_{ij}/2\,}. \tag{24}$$

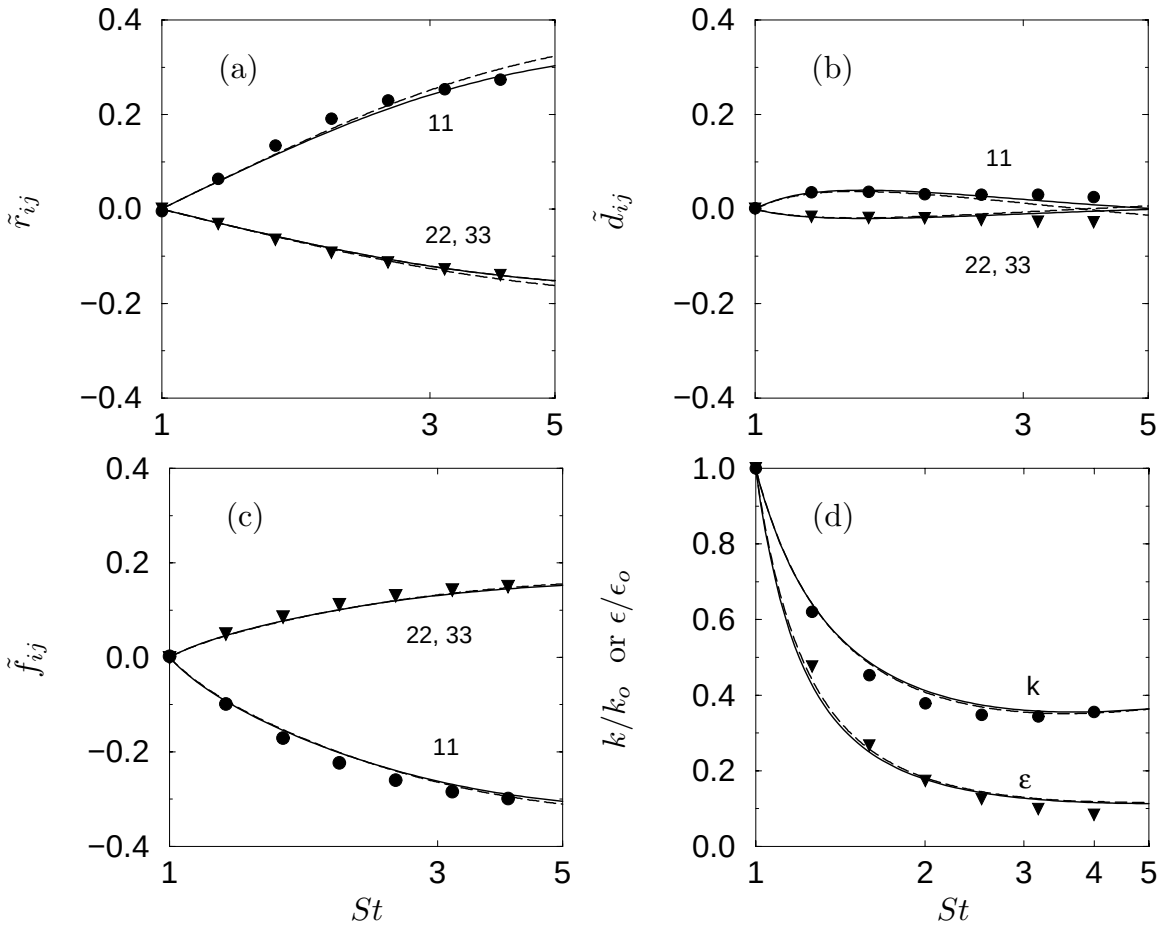

FIGURE 1. Comparison of the one-point Q-model predictions (– – – –) with the IPRM results (———) and the 1985 DNS of Lee & Reynolds (symbols) for the axisymmetric expansion case EXO ($Sq_0^2/\epsilon_0 = 0.82$). (a)-(c) evolution of the Reynolds stress, dimensionality, and circulicity anisotropies; 11 component (•), 22 and 33 components (▼). (d) evolution of the normalized turbulent kinetic energy (•) and dissipation rate (▼).

As was discussed in Kassinos & Reynolds (1996, 1997), the axisymmetric expansion flows exhibit a paradoxical behavior where a slower mean deformation rate produces a stress anisotropy that exceeds the one produced under RDT for the same total mean strain. This effect is triggered by the different rates of return to isotropy in the $\tilde{\mathbf{r}}$ and $\tilde{\mathbf{d}}$ equations, but it is dynamically controlled by the rapid terms. The net effect is a growth of $\tilde{\mathbf{r}}$ in expense of $\tilde{\mathbf{d}}$, which is strongly suppressed. The one-point model (see Fig. 1) is able to capture these effects well and also predicts the correct decay rates for the normalized turbulent kinetic energy k/k_0 and dissipation rate ϵ/ϵ_0. The predictions of the one-point Q-model are comparable to those of the nonlocal IPRM.

The case of homogeneous turbulence deformed by slow plane strain ($Sq_0^2/\epsilon_0 = 1.0$) is shown in Fig. 2. In this case the mean strain tensor is

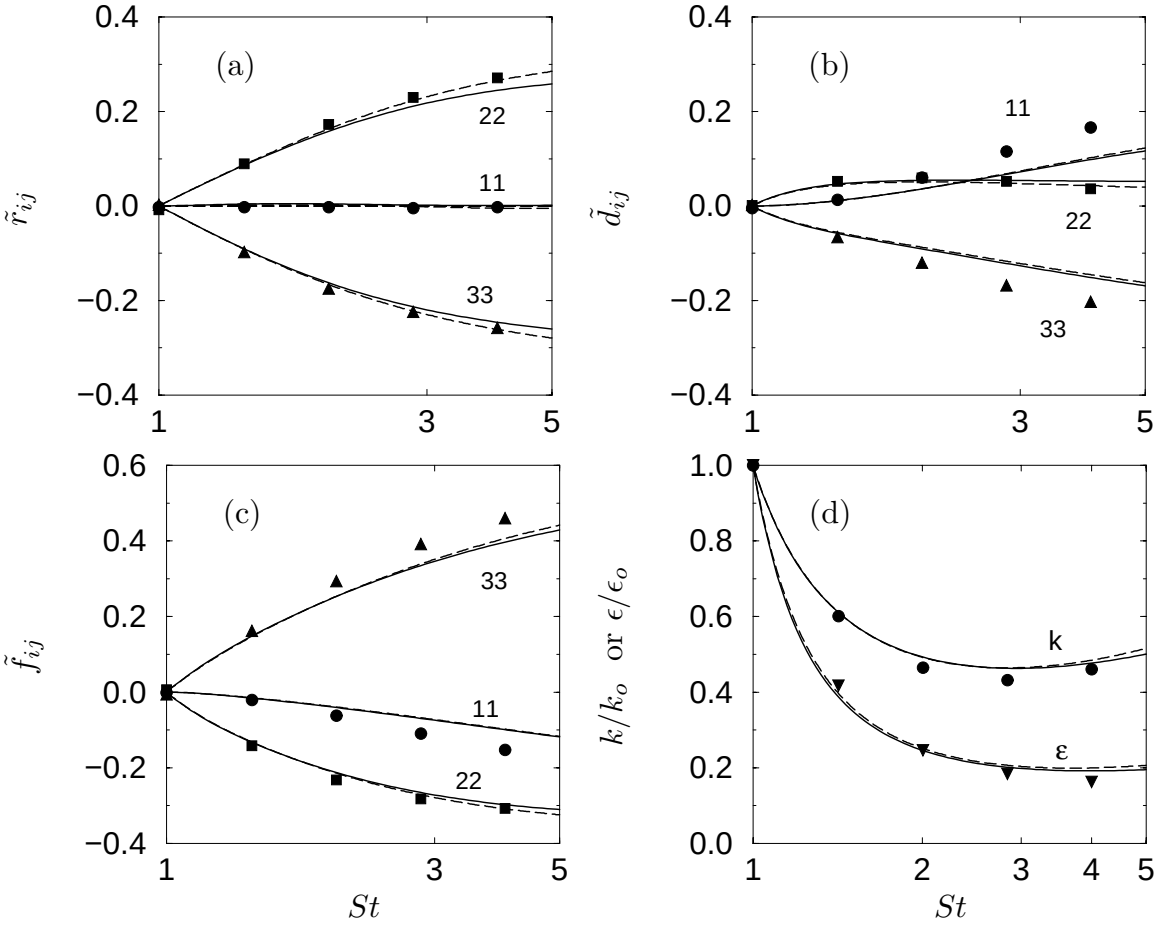

FIGURE 2. Comparison of the one-point Q-model predictions (– – – –) with the IPRM results (———) and the 1985 DNS of Lee & Reynolds (symbols) for the plane strain case PXA ($Sq_0^2/\epsilon_0 = 1.0$). (a)-(c) evolution of the Reynolds stress, dimensionality, and circulicity anisotropies; 11 component (●), 22 component (■), 33 component (▲). (d) evolution of the normalized turbulent kinetic energy (●) and dissipation rate (▼).

$$S_{ij} = S \begin{pmatrix} 0 & 0 & 0 \\ 0 & -1 & 0 \\ 0 & 0 & +1 \end{pmatrix} . \tag{25}$$

Again the performance of the one-point model is comparable to that of the IPRM, and its predictions compare favorably with the DNS results of Lee & Reynolds (1985). The details in the evolution histories of $\tilde{r}_{ij}$, $\tilde{d}_{ij}$ and $\tilde{f}_{ij}$ are captured, and the correct rates are predicted for the decay of the (normalized) turbulent kinetic energy k/k_0 and dissipation rate ϵ/ϵ_0.

The predictions of the one-point Q-model for the case of homogeneous shear are shown in Fig. 3. Comparison is made to the DNS results of Rogers & Moin (1987).

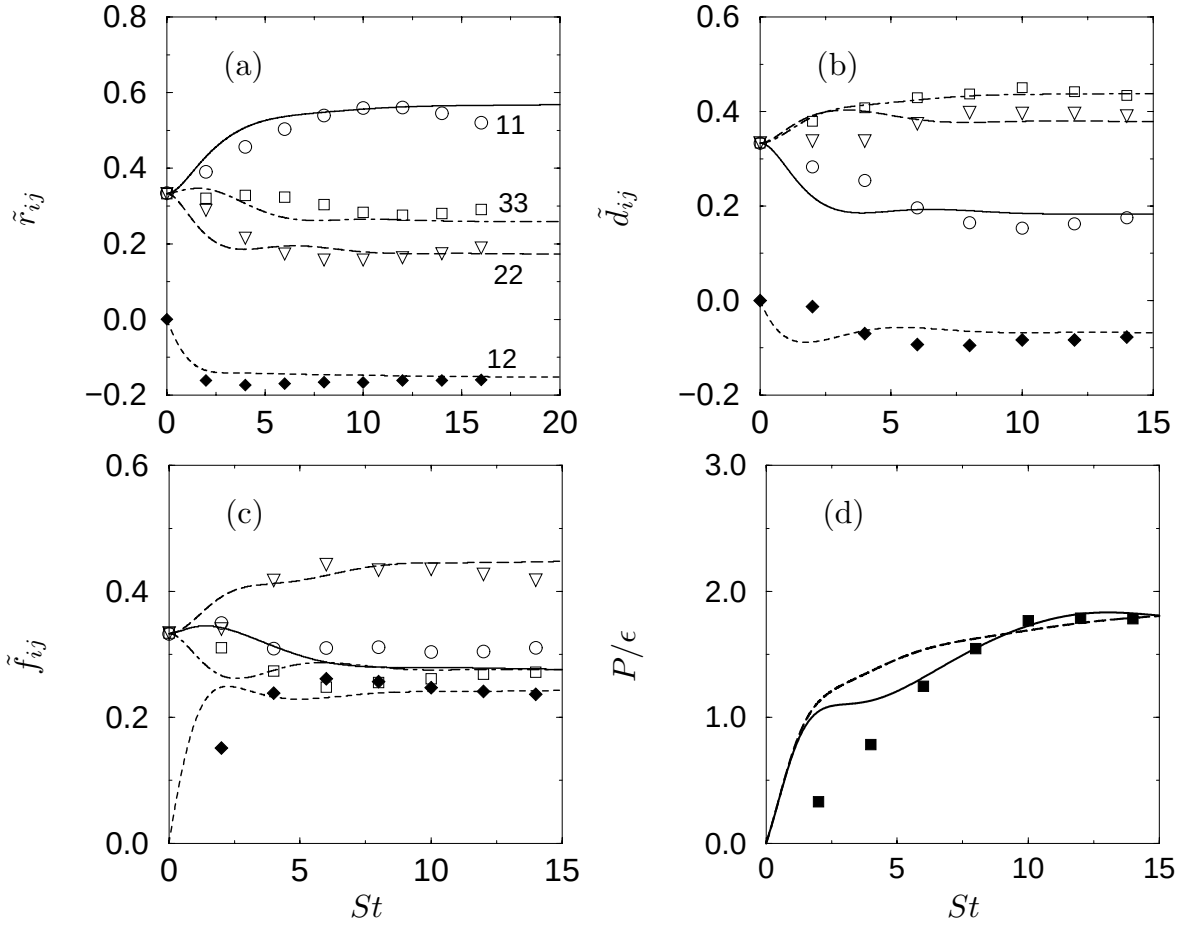

FIGURE 3. Comparison of the one-point Q-model predictions (lines) and the 1986 DNS of Rogers & Moin (symbols). (a)-(c) evolution of the Reynolds stress, dimensionality, and circulicity components in homogeneous shear with $Sq_0^2/\epsilon_0 = 2.36$: 11 component, (——— , ○); 22 component, (– – – – , ▽); 33 component, (—·— □); 12 component, (– – – – ,, ♦). (d) evolution of production over dissipation rate (P/ϵ): model, (– – – –); IPRM, (———); DNS (■).

Note that the model produces satisfactory predictions for the components of $r_{ij} = R_{ij}/q^2$, $d_{ij} = D_{ij}/q^2$, $f_{ij} = F_{ij}/q^2$. A fully-developed stage was reached in the simulations for $10 \leq St \leq 15$, and in this range both the Q-model and the IPRM predict the correct level for the dimensionless ratio of production over dissipation, P/ϵ.

A difficult challenge for one-point models is provided by the elliptic streamlines flows (see Fig. 4),

$$G_{ij} = \begin{pmatrix} 0 & 0 & -\gamma - e \\ 0 & 0 & 0 \\ \gamma - e & 0 & 0 \end{pmatrix} \qquad 0 < |e| < |\gamma| \tag{26}$$

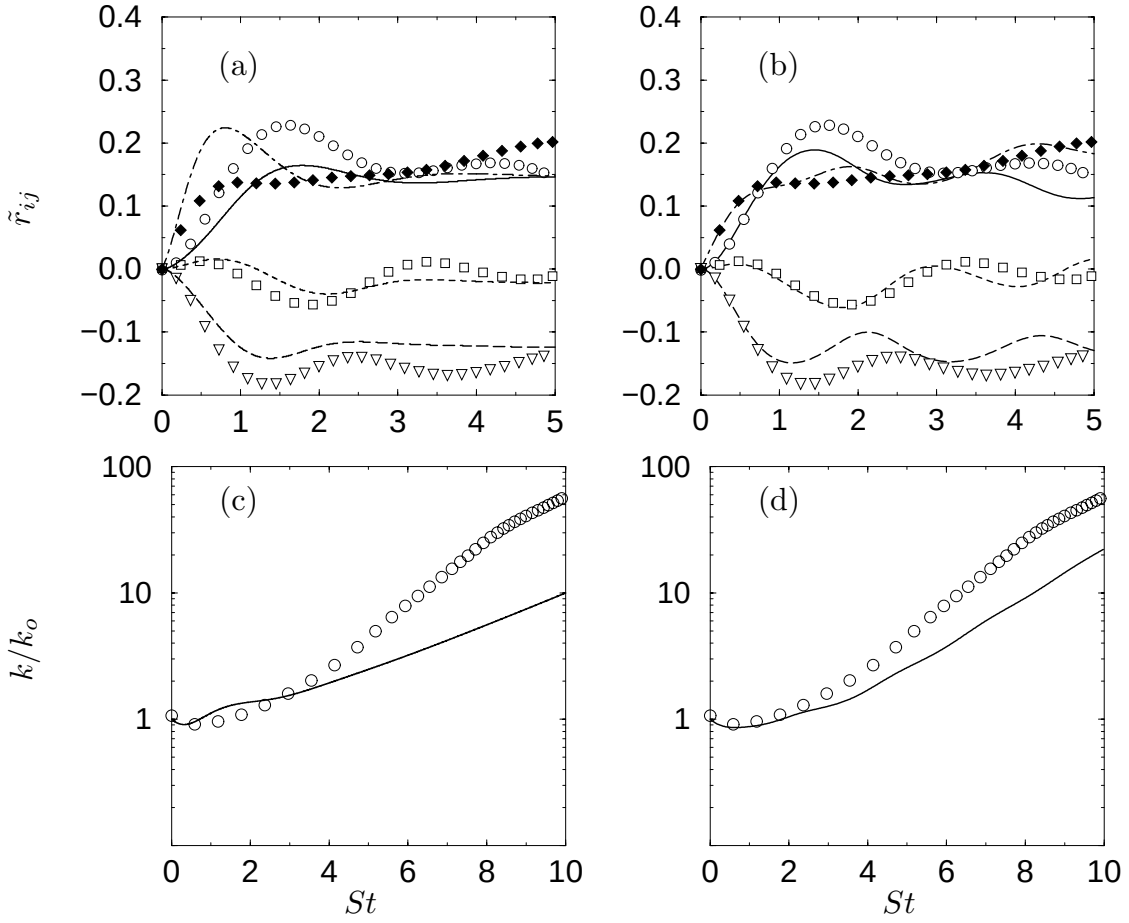

FIGURE 4. Comparison of model predictions (lines) for the evolution of the Reynolds anisotropy in elliptic streamline flow (E=2.0) with the 1996 DNS of Blaisdell (symbols). (a) one-point Q-model vs DNS, (b) IPRM vs DNS: 11 component, (——— , ○); 22 component, (- - - - , ▽); 33 component, (- - - - , □); 13 component, (—·— , ♦). Growth of the normalized turbulent kinetic energy: (c) one-point Q-model (line) vs DNS (symbols), (d) IPRM (line) vs DNS (symbols).

which combine the effects of mean rotation and plane strain and emulate conditions encountered in turbomachinery. (Note that the case $e = 0$ corresponds to pure rotation while the case $|e| = |\gamma|$ corresponds to homogeneous shear).

Direct numerical simulations (Blaisdell & Shariff 1996) show exponential growth of the turbulent kinetic energy in elliptic streamline flows, which analysis shows is associated with instabilities in narrow wavenumber bands in wavenumber space. Standard k-ϵ models as well as most RST models instead predict decay of the turbulence.

As shown in Fig. 4, both the one-point Q-model and the IPRM predict exponential growth of k. The rate of growth of k predicted by the one-point model is lower than those predicted by the IPRM and DNS but probably satisfactory for most purposes. In addition, the one-point model predicts the details of the evolution of

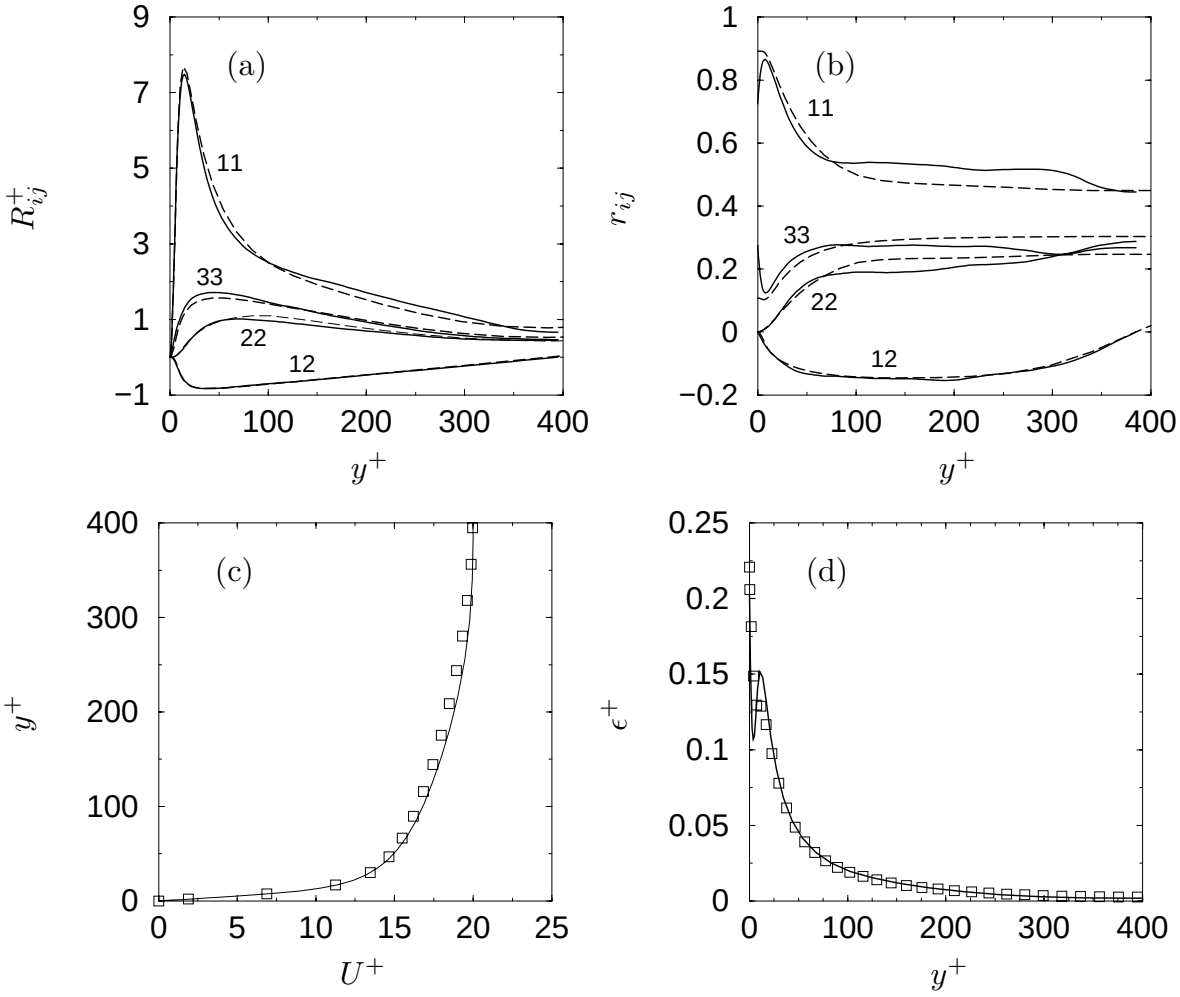

FIGURE 5. Comparison of model predictions with DNS (Mansour, 1998) for fully developed channel flow at $Re_\tau = 395$. (a) components of the Reynolds stress tensor, (b) components of the Reynolds stress tensor normalized by its trace: model, (———); DNS (- - - -). (c) mean velocity profile, (d) dissipation rate profile: model, (———); DNS, (□).

the Reynolds stress anisotropy components with a level of accuracy comparable to the IPRM, which again seems adequate for many engineering purposes, especially since none of the currently available k-ϵ and RST models can predict the elliptic streamlines flows at this level of accuracy and detail.

2.5 Extensions to inhomogeneous flows

The Q-model has been implemented in a 1D code and is currently being tested for fully developed channel flow. Inhomogeneous effects are accounted for through the addition of standard gradient diffusion models in the Q_{ijk} and ϵ equations. In other words in the evolution equations for the turbulent statistics, we allow for turbulent transport in a diffusion-like manner

$$\frac{DQ_{ijk}}{Dt} = \ldots + \frac{\partial}{\partial x_r}\big([\nu\delta_{rs} + \frac{C_\nu}{\sigma_{_Q}} R_{rs}\tau]\frac{\partial Q_{ijk}}{\partial x_s}\big) \tag{25}$$

$$\frac{D\epsilon}{Dt} = \ldots + \frac{\partial}{\partial x_r}\big([\nu\delta_{rs} + \frac{C_\nu}{\sigma_\epsilon} R_{rs}\tau]\frac{\partial \epsilon}{\partial x_s}\big)\,. \tag{26}$$

The turbulent kinetic energy is obtained from $k = \epsilon_{ikj}Q_{ijk}/2$.

Wall proximity effects and boundary conditions are treated through an elliptic relaxation scheme based on the ideas of Durbin (1993). Terms in the transport equation for Q_{ijk} which are assumed to represent nonlocal effects are lumped together into a term $\wp_{ijk}$, which is then replaced by a new tensor, $q^2 f_{ijk}/2$, obtained through an elliptic relaxation scheme

$$L^2\nabla^2 f_{ijk} - f_{ijk} = -2\wp_{ijk}/q^2\,. \tag{27}$$

The elliptic relaxation scheme allows the imposition of boundary conditions that produce the correct near-wall behavior for various components of Q_{ijk}. Away from the wall (27) allows one to recover the homogeneous model. This is in analogy to the elliptic relaxation scheme applied to RST models by Durbin.

Representative results for fully developed channel flow

Preliminary results obtained with the Q-model for fully developed channel flow are encouraging. The model was implemented in a 1D-code using elliptic relaxation as outlined above and with no wall-function treatment. A comparison of the Q-model predictions with DNS data (Mansour 1998) for fully developed channel flow at $Re_\tau = 395$ is shown in Fig. 5.

The Reynolds stress components (nondimensionalized with the wall shear velocity u_τ) are shown in Fig. 5a. The agreement between the model predictions (dashed lines) and the DNS (solid lines) is satisfactory. The model slightly overpredicts the peak in the streamwise component R_{11}^+ that occurs at about $y^+ \approx 15$. The components of the normalized Reynolds stress tensor $r_{ij} = R_{ij}/q^2$ are shown in Fig. 5b. The agreement between the model predictions and the DNS results is again reasonable. The agreement in the case of the shear stress r_{12} is noteworthy.

The mean velocity profile is shown Fig. 5c. The model prediction is in good agreement with the DNS profile, the most notable difference being in the value of the mean velocity in the log region.

Finally, the model profile of the dissipation rate ϵ is shown in Fig. 5d. The model is again in good agreement with the DNS but has a larger wiggle near the wall than the data show. This difference depends on the model transport equation for ϵ, and we are currently exploring alternative formulations that aim at taking full advantage of the structure information carried in the new model.

Future plans

The performance of standard RST models in flows with strong rotation is often compromised by their incomplete treatment of key physics in rotated turbulence. The new Q-model is based on a more rigorous treatment of rotational effects and offers the possibility to improve our predictive capabilities in strongly rotated turbulence. Hence, our immediate plans include the implementation and testing of the model in rotating wall-bounded flows, including rotating channel flow (with rotation either about the spanwise or streamwise direction) and axially rotating pipe flow. These cases will provide the first real test of the new model in flows where it is expected to perform better than standard closures.

REFERENCES

Blaisdell, G. A. & Shariff, K. 1996 Simulation and modeling of the elliptic streamline flow. *Proceedings of the 1996 Summer Program*, Center for Turbulence Research, NASA Ames/Stanford Univ., 433-446.

Durbin, P. 1993 A Reynolds-stress model for near-wall turbulence. *J. Fluid Mech.* **249,** 465-498.

Mahoney, J. F. 1985 Tensor and Isotropic Tensor Identities. *The Matrix and Tensor Quarterly.* **34(5),** 85-91.

Kassinos, S. C. & Reynolds, W. C. 1997 Advances in structure-based modeling. *Annual Research Briefs 1997*, Center for Turbulence Research, NASA Ames/Stanford Univ., 179-193.

Kassinos, S. C. & Reynolds, W. C. 1996 An Interacting Particle Representation Model for the Deformation of Homogeneous Turbulence. *Annual Research Briefs 1996*, Center for Turbulence Research, NASA Ames/Stanford Univ., 31-51.

Kassinos, S. C. & Reynolds, W. C. 1994 *A structure-based model for the rapid distortion of homogeneous turbulence.* Report TF-61, Thermosciences Division, Department of Mechanical Engineering, Stanford University.

Lee, M. J. & Reynolds, W. C. 1985 *Numerical experiments on the structure of homogeneous turbulence.* Report TF-24, Thermosciences Division, Department of Mechanical Engineering, Stanford University.

Mansour, N. N. 1998 Private communication.

Rogers, M. M. & Moin, P. 1987 The structure of the vorticity field in homogeneous turbulent flows. *J. Fluid Mech.* **176,** 33-66.